International Journal of Environmental Science and Technology (2020) 17:4465–4480
https://doi.org/10.1007/s13762-020-02789-8

ORIGINAL PAPER

Spatial evaluation of land-use dynamics in gold mining area using remote sensing and GIS technology

I. R. Orimoloye[1] · **O. O. Ololade**[1]

Received: 11 January 2020 / Revised: 3 May 2020 / Accepted: 28 May 2020 / Published online: 6 June 2020

Abstract

Gold mining operations generate a range of ecological and environmental impacts that can be measured spatially using geographic information system and remote sensing methods. This study assessed land-use and land-cover dynamics in the gold mining area using geographic information system and remote sensing techniques with the aid of Landsat 5 for years 1984, 1994, 2004 and Landsat 8 for 2014 and 2019 obtained from the United States Geological Survey and Remote Pixel Databases using ArcGIS 10.4 and R programming. The result from the study revealed the current changes and how they have evolved over the years where tailings dam and built-up areas increased from 90.5 to 172.9 km^2 between the year 1984 and 2019, while mine effluent (return water ponds) and water bodies increased from 14.7 to 18.8 km^2 during the same period. The area also experienced increased vegetation from 342.5 to 371.1 km^2 (though fluctuating during the study period) an indication that the area has witnessed revegetation in the area. Results from the study further revealed the vegetation health in the area utilises some vegetation indices such as the Global Environmental Monitoring Index, Normalised Difference Impervious Surface Index and Normalised Difference Moisture Index. Findings from the study show that areas with low index values are susceptible to the impact of mining and other anthropogenic activities, whereas high-index areas connote little or no impact. The outcome of this study provides a cost-effective tool for evaluating environmental impacts in mining areas that can drive policy interventions for remediation in affected areas.

Keywords Land-use dynamics · Mining activities · Environmental monitoring · Degraded area · Remote sensing

Introduction

Gold mining activities produce a range of ecological and environmental effects, many of which can be measured spatially using remote sensing (RS) and geographic information system (GIS) techniques. Mining is one of the human activities that can change an entire ecosystem, with several negative consequences such as contamination of surface water, groundwater and loss of biodiversity (Bebbington et al. 2008; Mudd 2010). However, abandoned mines with waste rock dumps and tailings reservoirs are distinguished from modern mine sites that have lower environmental impacts in comparison due to the improvements in operations and oversight by regulatory agencies.

RS and GIS have promoted or contributed to the mining and geological sectors immensely through explorations and environmental impact assessment research (Winde et al. 2019). Software developers and experts in the fields have also tailored RS and GIS applications to specifically meet the needs of mining operations and other industries (Granell et al. 2010; Werner et al. 2019). Most of the impacts of mining activities on the environment are detectable using earth observation data, for instance vegetation health, land and environmental degradation and landscape dynamics. However, some of the impacts are not easily assessable by remote sensing such as soil chemistry, water pollution and other chemical and biological properties. Therefore, different mining impacts, especially on the environment, require different methods. RS and GIS have been used widely in previous studies to determine environmental degradation or

Editorial responsibility: M. Abbaspour.

Electronic supplementary material The online version of this article (https://doi.org/10.1007/s13762-020-02789-8) contains supplementary material, which is available to authorised users.

✉ I. R. Orimoloye
orimoloyeisrael@gmail.com

[1] Centre for Environmental Management, University of the Free State, Bloemfontein, South Africa

landscape dynamics from satellite data of medium and high spatial resolution from different satellite sensors. Many of these findings from the studies have been integrated into operational exploration models based on GIS technology, which plays a significant role in decision-making in mineral exploration in selecting appropriate areas (Bonham-Carter 1994; Porwal and Carranza 2015). In addition to the use of RS and GIS in mining-related studies, these techniques have been broadly utilised in various environment-related research, such as flood events (Adefisan et al. 2015), land-use change and spatial planning (Busayo et al. 2019), land surface thermal characteristics (Willie et al. 2019), environmental and socioeconomic risk issues (Chen et al. 2003; Mutukwa et al. 2019).

While GIS and RS are powerful tools to analyse the varied mining impacts, they remain underused. Consequently, this study seeks to evaluate the land-use change in a mining area using RS and GIS for three decades to assess environmental sustainability within mining operations. Post-mining landscape dynamics should be prioritised after mining operations have stopped in order to manage or mitigate the associated environmental impacts. Therefore, an approach can be used for efficient and continuous monitoring of mining sites to identify possible degraded and land-use dynamics and related restoration. Some of the negative environmental effects that gold mining can have include habitat destruction, water pollution, soil degradation and sinkhole formation, while positive impacts such as jobs and community development projects are also significant. Studies have urged increased attention to how advances in RS and GIS technology can more equitably help to bridge gaps between the perception and practice of environmental impact assessment (Li et al. 2013; Mutukwa et al. 2019). Overall, the use of GIS-based thematic mapping for potential environmental impact is effective because it provides a new approach to risk-based mapping which involves the spatiotemporal assessment and this will help in the decision-making process.

Continuous monitoring of mine sites provides useful data regarding changes in vegetation cover and the patterns of land use and land cover. An assessment of changes in vegetation as well as restoration impacts serves as some key indicators in evaluating the environmental change in degraded land caused by mining operations (Li et al. 2012; Karan et al. 2016). However, conventional forms of monitoring such as laboratory and field investigation that are used to appraise changes in vegetation health and cover require a higher labour force and significant time which are quite costly. These methods are suitable tools for the analysis of large volumes of geographic data, over multiple scales.

Mining-induced impacts include the adverse effects specific to gold and other minerals extraction. Such impacts include, but are not limited to, land subsidence, soil contamination from heavy metal and pollution or mine tailings, water contamination, water inundation, slope failure, released gas explosion, inhalation of dust and toxic gases, and abandoned facilities. To reduce or mitigate these adverse environmental impacts and risks associated with mining operations, an assessment of both the magnitude and level of impacts or hazards based on continuous spatial assessment is crucial. Therefore, this study aimed at assessing land-use dynamics in the gold mining area using RS and GIS techniques between 1984 and 2019 in the Welkom area of Free State Province, South Africa. Monitoring the temporal and spatial dynamics of land-use/land-cover change in mining regions is crucial to environmentally sustainable mining development and management. These techniques provide a more effective assessment of changes in land-use/land-cover dynamics, which are more accurate and require less labour force and time (Ololade et al. 2008).

Materials and methods

Description of the study location

This study is focused on the Welkom area, situated in the Matjhabeng Local Municipality in the Free State Province of South Africa (Fig. 1). This study assessed the gold mining activities in the area, which is one of the richest gold exploration areas in South Africa as well as other commodities such as uranium. Mining activities in the area include two deep level gold mines, surface and underground mining with accompanying infrastructures such as chemical laboratories, waste rock dumps, metallurgical plants, tailings storage facilities and evaporation dams. The area also hosts several other intensive mining activities and some of the oldest tailings dams (Maya et al. 2015). Another land use in the area is dominantly zoned for agriculture and residential purposes.

The study area comprises two mining fields which are Beatrix and Harmony Gold mines as presented in Fig. 1. Beatrix Mine is situated in the Magisterial District of Matjhabeng, at latitude − 28.00597 S and longitude 26.84668 E near the towns of Welkom and Virginia, some 240 km southwest of Johannesburg. The site is accessed via the N1 highway between Johannesburg and Kroonstad, and then via the R34. Geographically it is located in the Free State Goldfield and is the southernmost mine in the Witwatersrand Basin. Harmony Gold is located at latitude − 28.00716 S and longitude 26.738096 E, and it is the third-largest gold mining company located in Welkom. The area is mostly covered by non-arable, moderate potential grazing land as well as marginal potential arable land. The Welkom region is among the top maize producing areas in South Africa which cover with about 19% and 13% of agricultural (farmland and newly cultivated land or sparse vegetation) and built-up area, respectively, in year 2019. Welkom

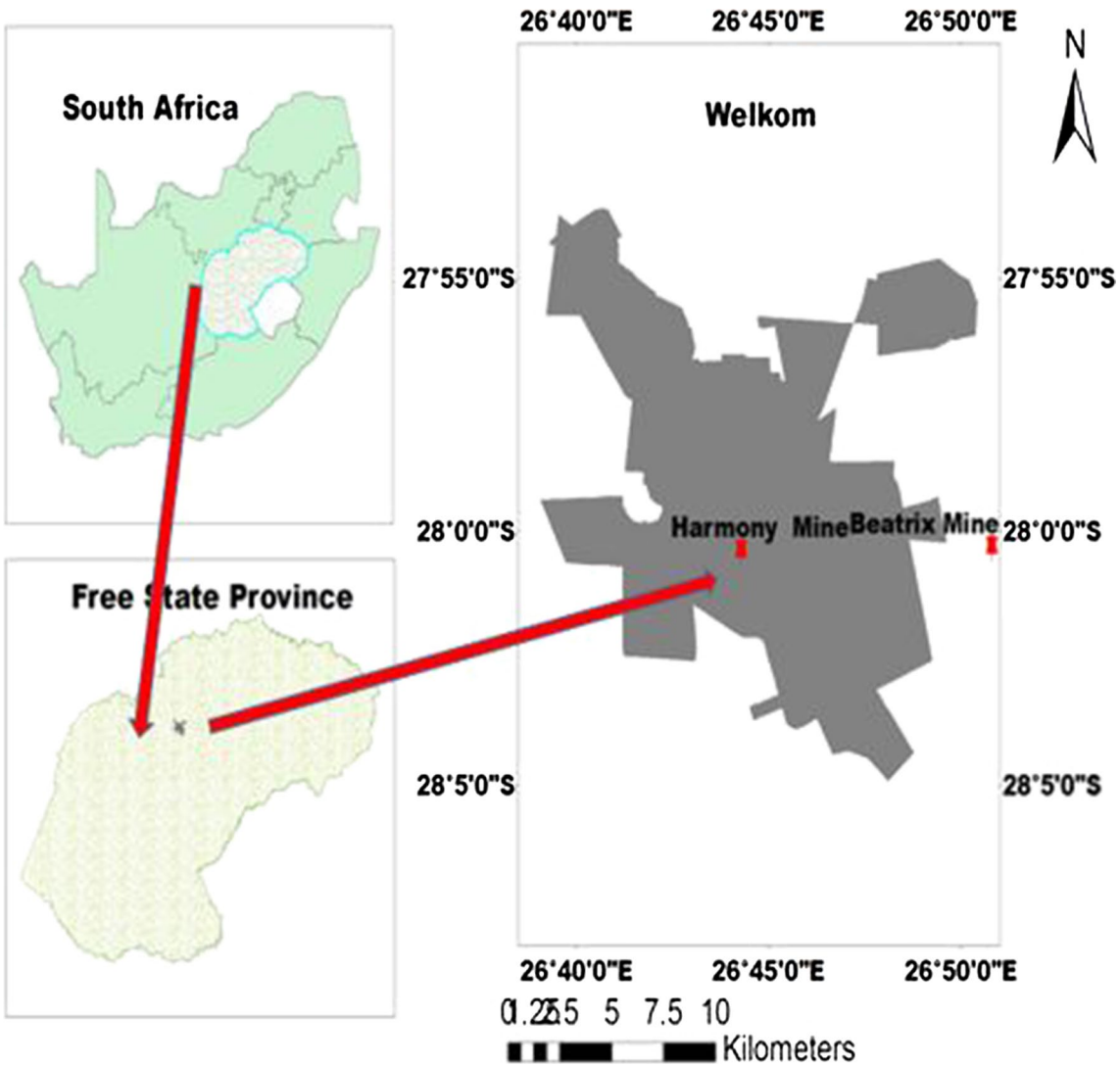

Fig. 1 Study location

usually receives around 401 mm–550 mm of rain per annum, depending on rainy or dry periods, with most rainfall occurring mainly during midsummer. This area receives the lowest rainfall in July (0 mm) and the highest rainfall in January (70 mm). Daily mean temperatures are distributed monthly from 17° C in June to 29° C in January. The area experiences the coldest at night during June and July months.

Data

The present study is divided into two parts. The first part involves the analysis of the spatiotemporal variability of land-use and land-cover dynamics in the mining areas using a combination of approaches consisting of supervised hybrid classification method, the Global Environmental Monitoring Index (GEMI), the Normalised Difference Moisture Index (NDMI) and the Normalised Difference Impervious Surface Index (NDISI). The second part focused on finding the most appropriate technique and determining the relationship between land-use systems based on statistical analysis in order to monitor the vegetation cover change and other land-use types for three decades (1984–2019).

Landsat historical images from the Landsat 5 Thematic Mapper (TM) and Landsat 8 Operational Land Imager (OLI) and the Thermal Infrared Sensor (TIRS) were used in the study. The images were acquired from the database of the United States Geological Survey (USGS) Earth Resource Observation Data Centre. This database was selected because it has an extensive and continuous imagery archives, higher spectral and spatial resolution, quality, consistency, comparably low cost of acquisition and higher frequency of observation, an attribute which makes it suitable for vegetation and land dynamics monitoring and management. Based on the defined period in this analysis, Landsat 4 and 5

images covering the years (multi-temporal) 1984–2004 and Landsat 8 for 2014 and 2019 were used to estimate derived landscape dynamics information. The image quality was limited to cloud coverage of less than 10%. The features considered for selecting the acquired satellite images was based on their technical specifications, including temporal resolution, spatial resolution, spectral resolution, cloud cover, zenith/nadir angle, sun altitude, swath width and image size (Du et al. 2015; Mensah et al. 2017). S_1 Table illustrates the technical specification and satellite data information used in this study.

Methods

The techniques used in the study consist of image preprocessing and classification analysis. The methodology's image processing stage includes sub-setting, gap-filling spatial/spectral and atmospheric correction. The method of spatial sub-setting involved cropping out undesirable geographic areas that are not part of the study area. Spectral sub-setting was done to limit the application of the classification analysis to select bands of the satellite images used in this investigation. All the analysis was done using ArcGIS 10.4 and R programming.

A hybrid approach for supervised image classification techniques was adopted in this study. The approach involves the use of a supervised classification method to identify individual pixels to be classified by filtering the dataset for natural clusters. This approach helped to identify clusters of all pixels in the data, which were later used as a basis for comparing the actual dynamic land-use classes present in the study area by using land-cover change to create digitised preliminary training data. The details on ground-truth training and preliminary training data were used to display the training sites, which are representative samples in the image for each land feature category. Supervised classification method was conducted with the maximum likelihood classification (MLC), as adapted from Bayes theorem (Xie et al. 2016). It focused on the probability that a pixel with a particular feature vector belongs to a specific land-cover class based on the training of a visual classifier for five different categories of land-use and land-cover dynamic. The process uses a sorting feature to assign each pixel with the highest probability of the category. Class mean vector and covariance matrix are the main inputs to the function and were derived from the training data of a specific class (Perumal and Bhaskaran 2010). The land-cover and land-use classes used for the supervised maximum likelihood classification include mine tailing dams and built-up area, dense vegetation, mine effluent and water body, farmland and sparse vegetation, bare and impervious surface.

Vegetation and degraded area mapping using some selected indices

Global Environmental Monitoring Index (GEMI), Normalised Difference Impervious Surface Index (NDISI) and Normalised Difference Moisture Index (NDMI) were used to map vegetated and degraded areas. One of the most popular parameters that are used to monitor land-use dynamics and vegetation health with multispectral data is GEMI. Study has shown that it can be used precisely to delineate vegetation cover and in environmental monitoring (Gumma et al. 2015). RS and GIS techniques can help in measuring the property of land features in terms of moisture or wetness using Normalised Difference Moisture Index (NDMI) derived from near-infrared (NIR) band 4 and SWIR band 5 as given in Eq. 1.

$$\mathrm{NDMI} - \frac{\mathrm{NIR} - \mathrm{SWIR}_1}{\mathrm{NIR} + \mathrm{SWIR}_1} \tag{1}$$

where SWIR_1 is band 5 and band 6 in Landsat 5 and Landsat 8, respectively.

Studies have shown that NDMI is highly correlated with water content and can, therefore, track changes in vegetation health and stress more closely than Normalised Vegetation Index (Hardisky et al. 1983). In heterogeneous environments, NDMI has an effective delineation of moisture content (Bolton and Friedl 2013; Chen et al. 2013).

GEMI is estimated from red and near-infrared bands. The formula was modified from Pinty and Verstraete (1992) as shown in Eq. 2:

$$\mathrm{GEMI} = \delta(1 - 0.25\delta) - \frac{(\rho\mathrm{RED} - o.125)}{(1 - \rho\mathrm{RED})} \tag{2}$$

δ is calculated using Eq. 3:

$$\frac{\delta = 2(\rho\mathrm{NIR}^2 - \rho\mathrm{RED}^2) + 1.5\rho\mathrm{NIR} + 0.5\rho E}{(\rho\mathrm{NIR} + \rho\mathrm{RED} + 0.5)} \tag{3}$$

The NDISI takes advantage of distinctive variations in spectral response between impervious materials and other land features. Most impervious surfaces tend to have high daytime thermal band response values (Li et al. 2011) and relatively low visible, near-infrared (NIR) and middle-infrared (MIR) reflectance values (Liu et al. 2013). The NDISI is thus evaluated by Eq. 4:

$$\mathrm{NDISI} = \frac{T_{\mathrm{lst}} - [(R_{\mathrm{VIS}} + R_{\mathrm{NIR}} + R_{\mathrm{MIR}})/3]}{T_{\mathrm{lst}} + [(R_{\mathrm{VIS}} + R_{\mathrm{NIR}} + R_{\mathrm{MIR}})/3]} \tag{4}$$

where R_{NIR} and R_{MIR} reflect the NIR and MIR bands (e.g. Thematic Mapper (TM)/Enhanced Thematic Mapper Plus (ETM+) band 4 and band 5, respectively), R_{VIS} reflects one of the visible bands, for example TM/ETM+ band 1, 2 or 3, and T_{LST} represents the thermal band surface temperature

(e.g. TM/ETM + band 6). Before applying, all index elements are rescaled to 8-bit digital number (DN) values.

The correlation coefficients of different land feature dynamics

This study assesses the relationship between various land-use and land-cover dynamics in the study area and highlighted their statistical significance (Howell 2002). Pearson's coefficient was evaluated using the algorithm below (Eq. 5):

$$r = \frac{\sum_{i=1}^{n}(x_i - \bar{x})(y_i - \bar{y})}{\sqrt{\sum_{i=1}^{n}(x_i - \bar{x})^2 \sum_{i=1}^{n}(y_1 - \bar{y})^2}} \quad (5)$$

Kendall's γ can be used with any variables that are at least ordinal. Each pair of data points is classified as concordant, discordant or tied (Howell 2002). When both variables increase and decreases, it is concordant; it is discordant when one variable increases and the other one decreases; and it is tied when one or both variables stay constant. C, D and T represent the number of concordant, discordant and tied pairs. The Kendall's coefficient is given by:

$$\gamma = \frac{C - D}{N} \quad (6)$$

where $N = C + D + T$ (the total number of land-use/land-cover categories). The correlation coefficients analysis of the different land-cover dynamics was performed using R programming.

Parameters accuracy

The hybrid technique was adopted to increase the overall accuracy of the classification. Accuracy assessment quantifies how best classification was carried out by the classifier which is the validation process performed by comparing results of the analysis and the actual ground-truth referenced information that accurately represents the true land-use/land-cover dynamics of the concerned area (Brabyn et al. 2014). Hence, the accuracy assessment is a measure of the disparity between the results of the spatial analysis and the referenced data. Based on this fact, highly accurate reference data randomly distributed across the study area are chosen for evaluation, thus taking into account the temporal significance of the reference data for the overall accuracy evaluation of the result (Mensah et al. 2017).

Results and discussion

This study presents land-use and land-cover dynamics in the study area between 1984 and 2019 using RS and GIS techniques. The result of the study shows the current condition and how the changes have evolved over the years. Figure 2 gives an overview of the supervised classification of the study area between 1984 and 2019, and it is provided in accordance with the land coverage for the different land characteristics obtained from the image and vegetation indices used for tracking environmental degradation as well as mine-degraded areas. The areas covered by different land characteristics were evaluated including tailings dam and built-up areas, mine effluent and water bodies, dense vegetation, farmland and sparse vegetation, and bare and impervious surfaces (newly cultivated area, sand fill, open ground and rock).

In the year 1984, the area covered by bare and impervious surfaces was about 499.469 km^2 followed by farmland and sparse vegetation with 348.530 km^2. Dense vegetation, tailings dam and built-up, and effluent and water bodies covered about 342.47, 90.54 and 14.71 km^2, respectively, in the same year. Different land features emerged in the year 1994 where farmland and sparse vegetation covered the highest land area with about 634.16 km^2 followed by bare and impervious surface and dense vegetation with about 476.64 and 90.47 km^2, respectively, in the same year. Tailings dam and built-up and mine effluent and water bodies covered about 81.35 and 13.10 km^2, respectively (Fig. 2a, b). The disparities in land-use/land-cover dynamics over the study area in the first 10 years revealed that the area has witnessed environment-related imbalances with a drastic increase in farmland and unhealthy vegetation as well as a decrease in densely vegetated areas. This development connotes that there may be other external factors responsible for this variability; for instance, deforestation and increased population might have played a vital role in this degradation (Glantz 2019).

The result from the study also revealed more changes in land dynamics in the year 2004 where dense vegetation had the highest land use/land cover with about 501.43 km^2 followed by a bare and impervious surface with about 429.48 km^2; tailings dam and built-up area covered about 211.67 km^2. Farmland and sparse vegetation, tailings dam and built-up, and mine effluent and water bodies covered 142.70, 211.67 and 10.44 km^2, respectively, in the same year. In the year 2014, there was a significant increase in farmlands and sparsely vegetated areas, tailings and built-up areas, effluent and water bodies with about 836.30 and 260.23 km^2, respectively. Dense vegetation and bare and impervious surfaces declined in extent with about 73.01, 11.83 and 9.34 km^2, respectively, in the same year. Finally, in the year 2019, there was an increase in bare and impervious surfaces, farmland and sparse vegetation, dense vegetation, mine effluent and water bodies with about 481.08, 251.75, 371.12 and 18.85 km^2, respectively. There was a significant increase in both vegetated and mine tailings and settlement areas because of the decrease in bare and impervious surfaces between 1984 and 2019 due to mining

Fig. 2 **a** Land-use and land-cover change between 1984 and 2019, **b** pie chart showing the percentage of land feature dynamics (1984–2019)

operations and urban growth (Sebego et al. 2019). The increase in vegetated areas can be attributed to the recent cessation in mining operations in the area and revegetation of bare and impervious surfaces (Fig. 3).

Only about 19% of the sparse vegetation and farmland cover of 1984 exists in 2019 with about 18% direct loss to the bare and impervious surface and about 1% increase in mine effluent and water body in the year 2019 with 1% cover area.

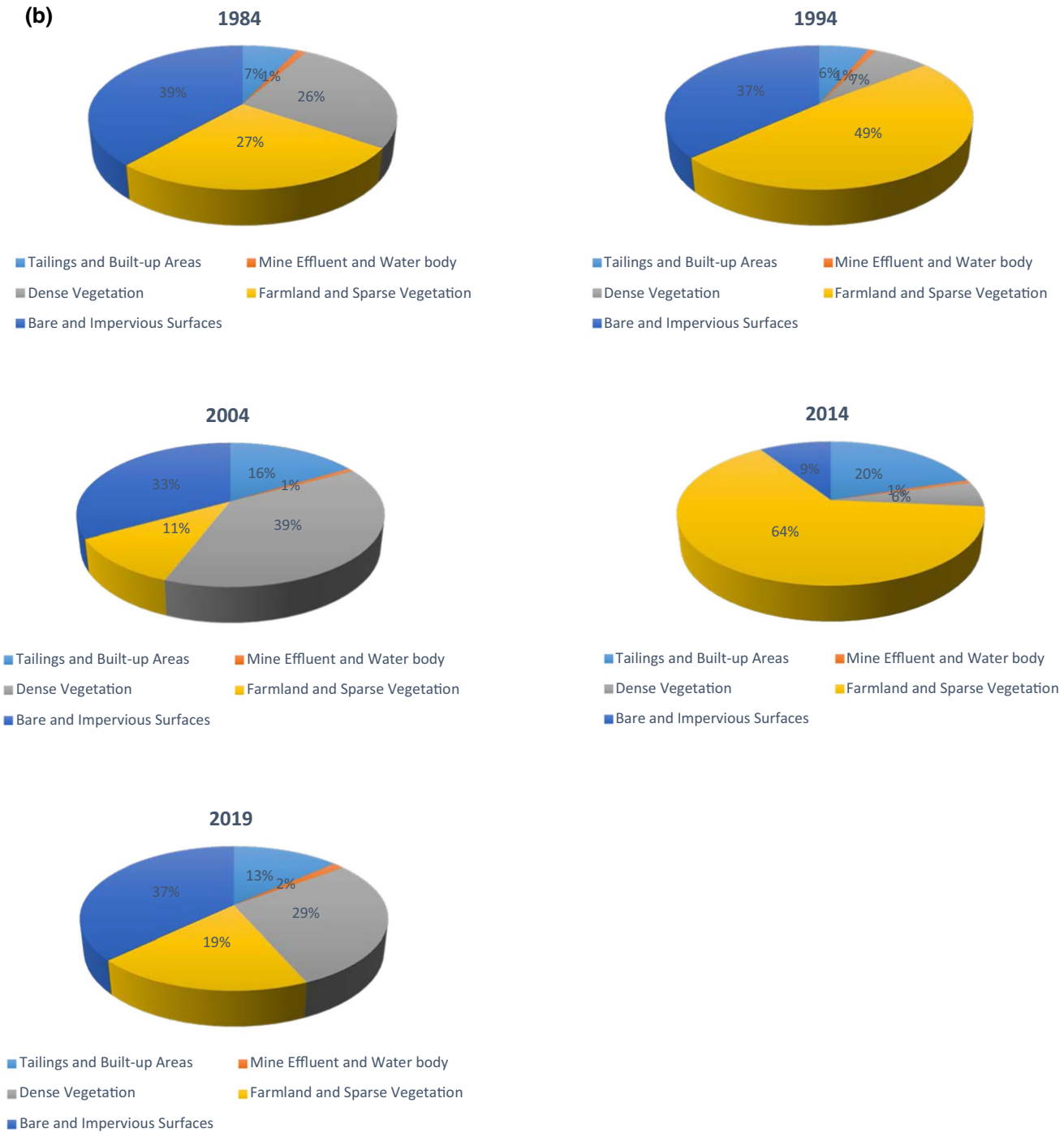

Fig. 2 (continued)

However, farming and other anthropogenic activities might have also contributed to the land-use/land-cover dynamics in the area, with mining activities accounting for a significant change in natural land cover and surface water (Li et al. 2016; Sebego et al. 2019). Tailings dam and built-up areas underwent some increases in the area covered with about 7% and 13% in the year 1984 and 2019, respectively. However, there are some situations where the land features experienced fluctuations in area extent, probably due to seasonal and climatic factors. For example, if the precipitation amount is below normal in a particular year, it can contribute to the decline in vegetation abundance (Li et al. 2016; Hou et al. 2019). The result from the study also highlights that there was an increase in vegetation cover during the period of investigation, whereas

Fig. 3 Vegetated area (obtained during fieldwork, September 2019)

other land features have various dynamic patterns during the same period. The fluctuations in the natural land-cover classes especially vegetation between 1984 and 2019 show that various factors may be responsible for the changes such as climate change, deforestation, built-up and other human activities including mining (Li et al. 2016; Liu et al. 2015). These significant impacts on the natural land-cover classes in the study area need proper monitoring which is crucial for environmental sustainability and restoration.

As human activities including mining operations, shift farming, farmlands, urbanisation and deforestation increase, these will, in turn, have an adverse effect on the natural environment as indicated in previous related studies (Ololade et al. 2008; Xie et al. 2016; Orimoloye and Ololade 2020a). The environmental liabilities caused by mining, expansion of agriculture and urbanisation needs to be properly monitored and assessed to create awareness on the extent of degradation and destruction within the mining environment (Xie et al. 2016, 2017). Long after mining operations have ceased, the land in the area is most often abandoned to revegetate naturally; however, this practice does not guarantee effective land restoration and rehabilitation. This study shows diverse changes in land systems in the area involving a continuous reduction in vegetation cover which may compromise ecosystem integrity with serious environmental impacts on the study area including a reduction in capacity to sequester carbon, susceptible to soil erosion, biodiversity losses, ecological imbalance and climatic changes (Mensah et al. 2017). This study further assesses and highlights the relationship between various land-use/land-cover systems in the study area as presented in Fig. 4a and b.

This study statistically appraised the relationship between land system dynamics using Kendall and Spearman correlations. These give a numerical summary of the degree of association between different land-use/land-cover categories used in this study. For instance, there is a negative degree of association between tailings dam and built-up area (TBA) and bare and impervious surface (BIS), which connotes that the TBA increases with decreases in BIS (Table 1). The correlation between mine effluent and water body (MEWB) and BIS is moderate and positively correlated with about 0.7, connoting that there is a moderate increase in mine effluents with an increase in bare and impervious surfaces as shown in Fig. 4 and Table 1. This increase in mine effluents can impose limitations on the usefulness of the freshwater resources in the area (Zhang et al. 2017). For instance, the acidic mine drainage from the goldfields interacting and causing deterioration of the water and soil quality can promote environmental degradation in the affected areas. The study further revealed that there exists a negative relationship between BIS and farmland and sparse vegetation (FSV) during the same period as shown in Fig. 2. This connotes that BIS decreases or increases with a decrease or increase in FSV in the study area during the same period. A correlation between dense vegetation (DV) and FSV shows that there exists a negative relationship between the two land feature categories in the area; an increase in farmland can contribute to a decline in dense vegetation. The spatiotemporal trends of vegetation or forest cover can be an indication of how healthy the environment is, with a decrease in vegetation and an increase in bare surface cover exacerbate environmental degradation. This could have a significant impact on human and environmental health in the area (Orimoloye et al. 2018; Orimoloye and Ololade 2020b).

Table 2 presents the Kendall and Spearman correlation coefficients for the land feature dynamics between 1984 and 2019. To support the general relationship between land-use/land-cover categories as discussed, this study employed Kendall and Spearman correlation coefficients to support the general correlation coefficient presented in Table 1. The result shows that TBA and BIS are negatively correlated with about − 0.6 Kendall coefficient, while TBA and MEWB are moderately negative correlated as

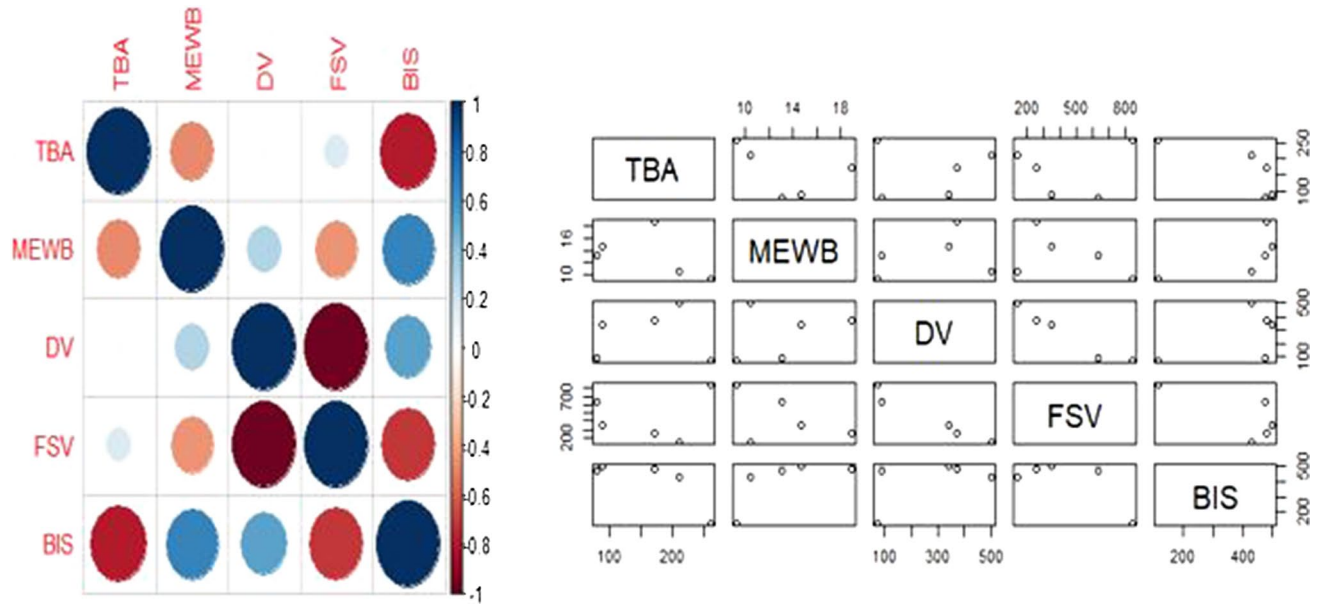

Fig. 4 Correlation of different land uses and land covers over the study area

Table 1 General coefficient for land-use dynamics

	TBA	MEWB	DV	FSV	BIS
TBA	1.00	−0.48	0.04	0.15	−0.78
MEWB	−0.48	1.00	0.29	−0.45	0.67
DV	0.04	0.29	1.00	−0.97	0.53
FSV	0.15	−0.45	−0.97	1.00	−0.71
BIS	−0.78	0.67	0.53	−0.71	1.00

Table 2 Kendall and Spearman correlation coefficients for land-use dynamics between 1984 and 2019

	Kendall				
	TBA	MEWB	DV	FSV	BIS
TBA	1.0	−0.4	0.2	−0.2	−0.6
MEWB	−0.4	1.0	0.4	−0.4	0.8
DV	0.2	0.4	1.0	−1.0	0.2
FSV	−0.2	−0.4	−1.0	1.0	−0.2
BIS	−0.6	0.8	0.2	−0.2	1.0
	Spearman				
TBA	1.0	−0.6	0.0	0.0	−0.7
MEWB	−0.6	1.0	0.4	−0.4	0.9
DV	0.0	0.4	1.0	−1.0	0.3
FSV	0.0	−0.4	−1.0	1.0	−0.3
BIS	−0.7	0.9	0.3	−0.3	1.0

depicted in the general correlation analysis (Table 1). The result revealed that MEWB and BIS are positively correlated during the same period. It further reveals a negative correlation between TBA and BIS using the Spearman coefficient, which also confirms the results of the general and Kendall correlations analysis. However, a positive correlation was observed between BIS and MEWB using the Spearman coefficient. Although gold mining has existed in the study area for decades, this study found evidence of a spatial association in the region between gold mines and vegetation and forest cover loss or fluctuation.

This result further shows the spatial pattern during the period of study (1984–2019) between gold mining and deforestation. Changes in the relationship between land use include gold mining activities and creation of agricultural concessions over the years are complex, but they appear to be closely linked to gold mining activities and other environmental factors, such as the weather patterns of the area (Zarin et al. 2004), with significant impacts on local communities. A study conducted by Zarin et al. (2004) states that forests are potential poverty and health traps, where vegetation dependency is correlated with less income-generating activities, resulting in a variety of negative social and economic outcomes (Zarin et al. 2004).

Spatiotemporal variation analysis of GEMI, NDMI and NDISI

This study used GEMI, NDMI and NDISI indices to assess the extent of environmental degradation in the area of investigation during the study period using space-based observation as presented in Figs. 5, 6 and 7. The information in Fig. 5 shows the state of the environment over the study period based on GEMI. The variation in the land characteristics and vegetation

health for the summer seasons are estimated and highlighted in Figs. 4, 5 and 6. The global monitoring index attempts to categorise the land surface by evaluating atmospheric conditions near the surface using earth observation information.

The impacts of mining activities on their immediate environment can be easily identified from the space-based observation and the visual visibility changes of Landsat 5 and 8 data. Figure 5 shows the spatial variation in vegetation cover and the potentially degraded areas due to gold mining

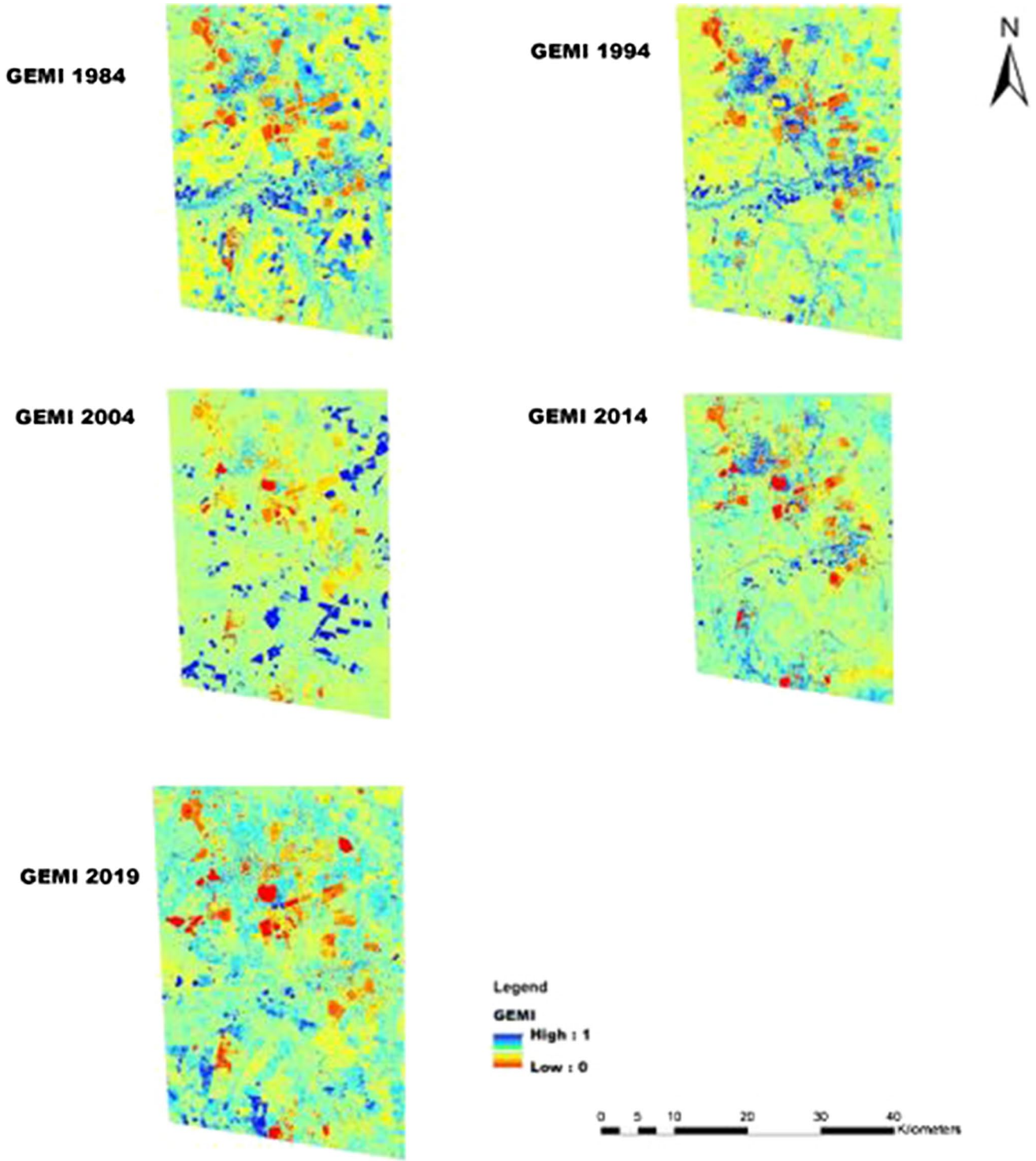

Fig. 5 Spatial analysis of Global Environmental Monitoring Index between 1984 and 2019

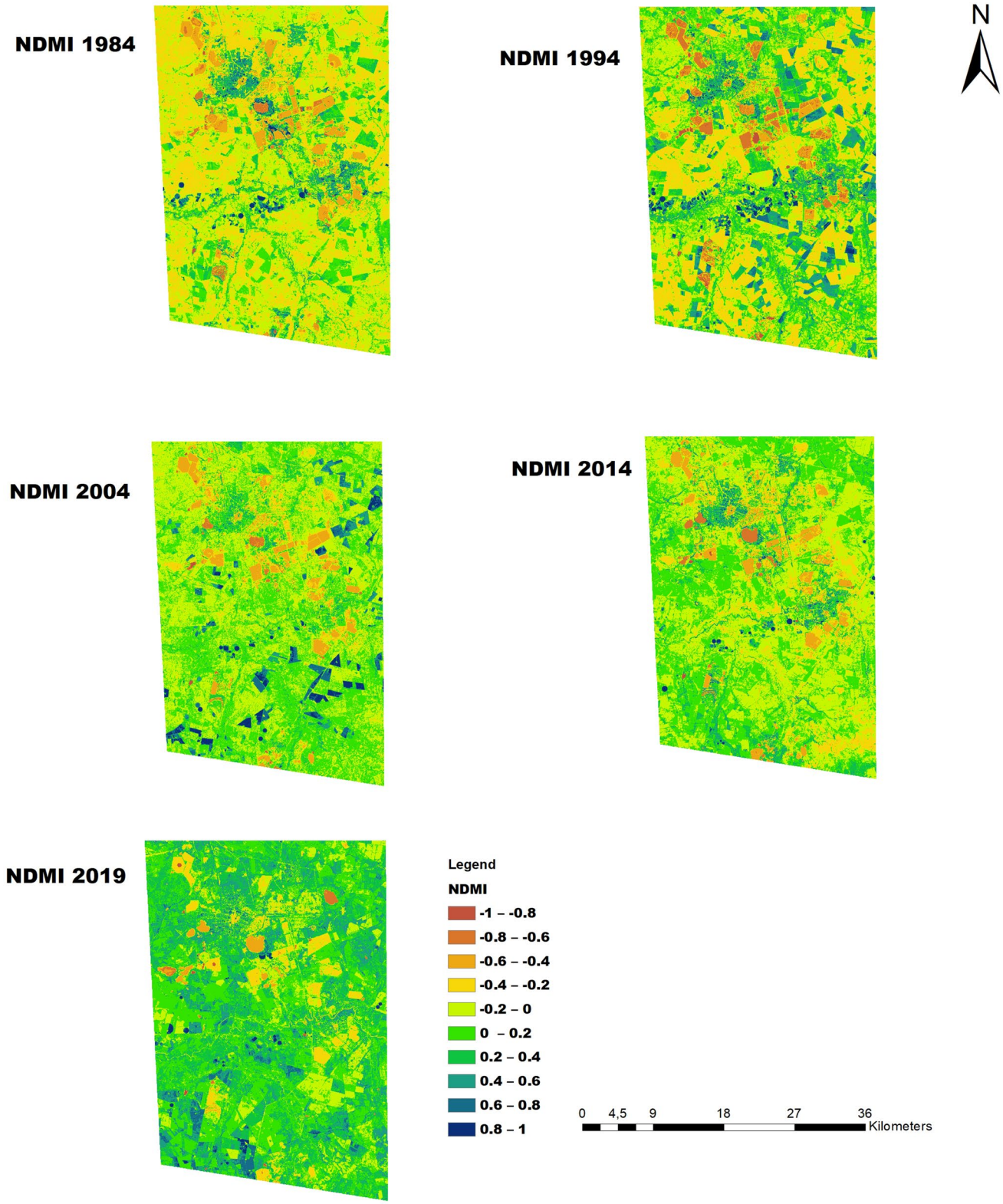

Fig. 6 Spatial analysis of Normalised Difference Moisture Index between 1984 and 2019

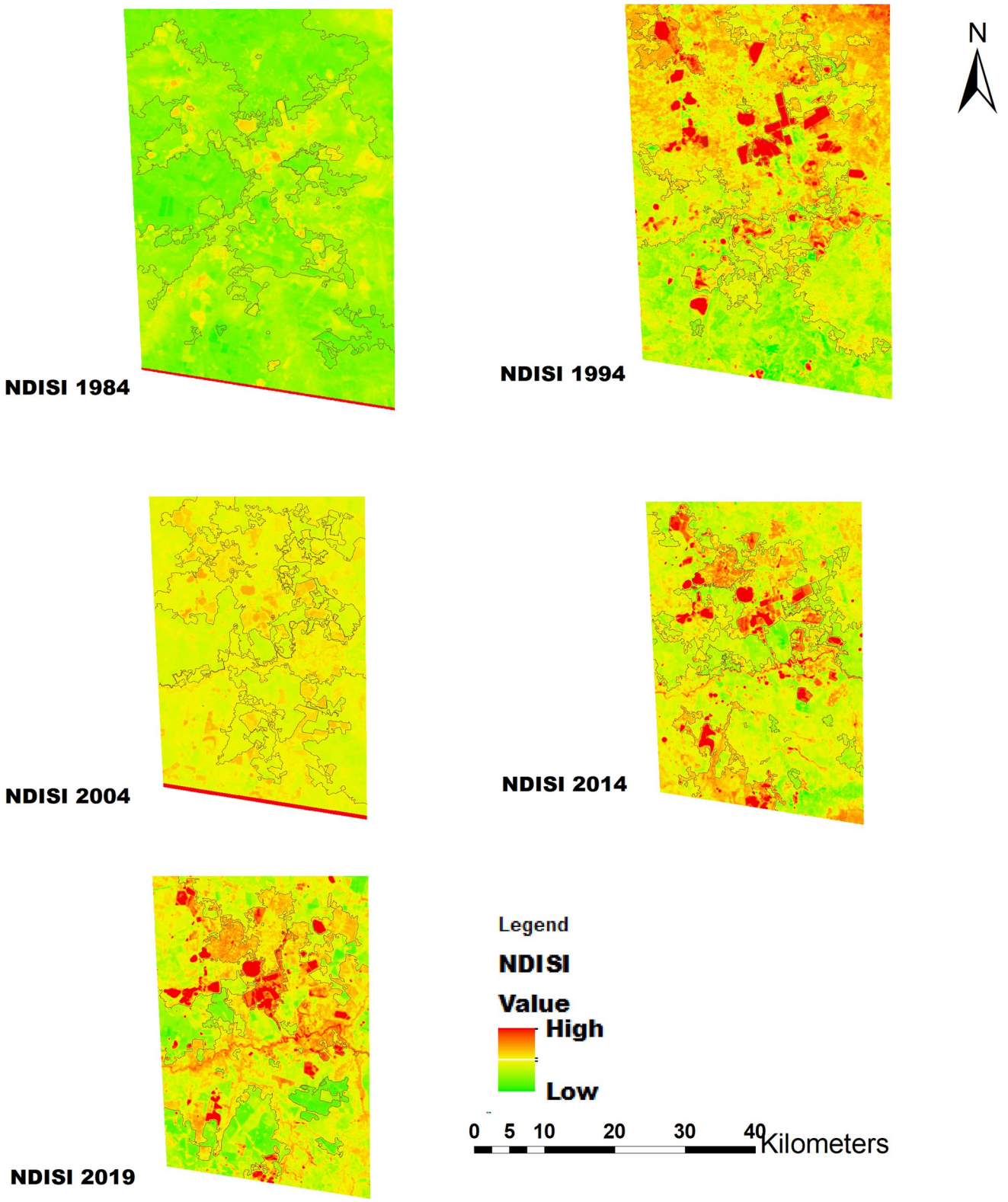

Fig. 7 Spatial analysis of Normalised Difference Impervious Surface Index between 1984 and 2019

and other anthropogenic activities where red and blue represent the high and low degraded areas, respectively. Taking into account the algorithm for generating NDMI, NDISI and GEMI, it is known that they are the most appropriate indices for analysing vegetation objects and environmental health status, open land (gold and soil outcrops), vegetation covers and water or moisture content. GEMI tends to be similar to Normalised Difference Vegetation Index, which is used to analyse vegetation cover for evaluating environmental degradation (Haryani et al. 2018).

Analysis of the 1984, 1994, 2004, 2014 and 2019 images shows the different spatial trends of GEMI over the study area. Findings from the analysis indicate that areas with low GEMI values are vulnerable to the effects of mining and other anthropogenic activities, whereas high-GEMI areas connote little or no impact incidence (Haryani et al. 2018). It was noted that in the years 1984, 1994 and 2004 the study area witnessed vegetation increase, while the reverse is the case in 2014 and 2019. This connotes that the areas that are susceptible to environmental degradation are less in the first two decades of the period of the study compared to the years 2014 and 2019 as presented in Fig. 5. This shows that the lack of regular on-site environmental impact monitoring of mining activities and its adverse effect on the immediate environment and related ecosystems could have contributed to the development and occurrence of any environmental degradation in the area (Haryani et al. 2018). Environmental impacts arising from mines in the study area are usually associated with open-pit mines, although underground mining operations could also cause changes in the landscape through alteration of the chemical, biological and physical properties of the soil, and may ultimately cause damage to the earth's surface (Sheoran et al., 2010). This condition can disrupt the ecosystem functioning in the affected areas (Glantz 2019).

The information in Fig. 6 presents a spatial pattern of Normalised Difference Moisture Index between 1984 and 2019. The NDMI defines the degree of soil or water stress and is measured in the near-infrared and SWIR as the ratio between the difference and the amount of the refracted radiation. This index helps to identify land or field areas with water stress issues. NDMI is easy to interpret with values varying from −1 to 1, each value corresponding to different agronomic or environmental situations, regardless of the surface water content of the soil (S_2 Table). The minimum and maximum NDMI values were evaluated to identify potential environmental impacts such as changes in vegetation and other environmental components in the study area. The interval is then divided into 10 groups, each corresponding to a different water-vegetative stress level with the land-cover areas where the NDMI was lower connotes vegetation stress (Glantz 2019). Studies have shown that the areas that are water or vegetation stressed have the potential to be more affected with a continuous or prolong depletion in vegetation cover (Glantz 2019).

Bare land/soil, very low canopy cover, low canopy cover, dry or very low canopy cover are highly vulnerable to erosion (Fig. 5). These are areas that were not covered by trees, debris or duff, fallen woody material or rocks. All these can contribute to both the removal of topsoil and the degradation of the mining area. In both cases, the quality of water could be affected as well as the loss of valuable soil and acreage. Soils that are not covered by required vegetation are prime areas where noxious weeds or other undesirable plant species invasions occur. Bare ground also raises the risk of reduction in the soil's water-holding capacity. While high canopy cover and very high canopy cover signify no water stress, total canopy cover connotes no water stress/waterlog, an indication that these areas have little or no vegetation stress. Based on the NDMI categories in S_2 Table and Fig. 5, the results show that there were low NDMI values in the years 1984 and 1994 in most parts of the study area. This meant that bare soil or surface, absent of canopy, and low canopy along with water stressed were present in the area during this period (S_2 Table and Fig. 5). This is because land degradation is considered as any sort of deterioration in soil quality that in one way or the other affects the coherence of biodiversity, in terms of reducing either their sustainable ecological sustainability or biological assets and ability to retain their resilience (Heggelund et al. 2005). In each case, land degradation has an adverse impact on different sectors, such as agriculture with major structural constraints on economic growth, human development and environmental sustainability. The result further revealed that in the years 2004, 2014 and 2019 there was a slight increase in canopy cover and low water stress in most parts of the study area. NDMI values over these years corroborate with the land-use/land-cover dynamics presented in Fig. 2, which shows an increase in vegetation cover in the area. This vegetation patterns could also be attributed to various factors, such as variability in rainfall events and climate change.

Figures 7 and 8 show the generated NDISI status of the study area. Several subsets are extracted from validation analysis, including various impervious land covers, built-up, open surface, rooftop and other related surfaces. A qualitative comparison suggests that the area with an impervious surface is effectively enhanced. In the NDISI results, both the transport and building roof-related impervious surfaces are shown with a light yellow to red hue. In addition, yellow to red pixels mainly appear in less vegetated zones and urban area, which connotes or represents the presence of the impervious surface. Green to blue pixels mainly appear in vegetated zones and suburban or city fringes, which connotes or represents the presence of less impervious surface (Beck et al. 2016). To further evaluate the suitability of NDISI, comparative analyses of NDISI trends for different years 1984, 1994, 2004, 2014 and 2019 (Fig. 8a–e) were conducted within this study. The result further confirmed that the year 1984 witnessed a low rate

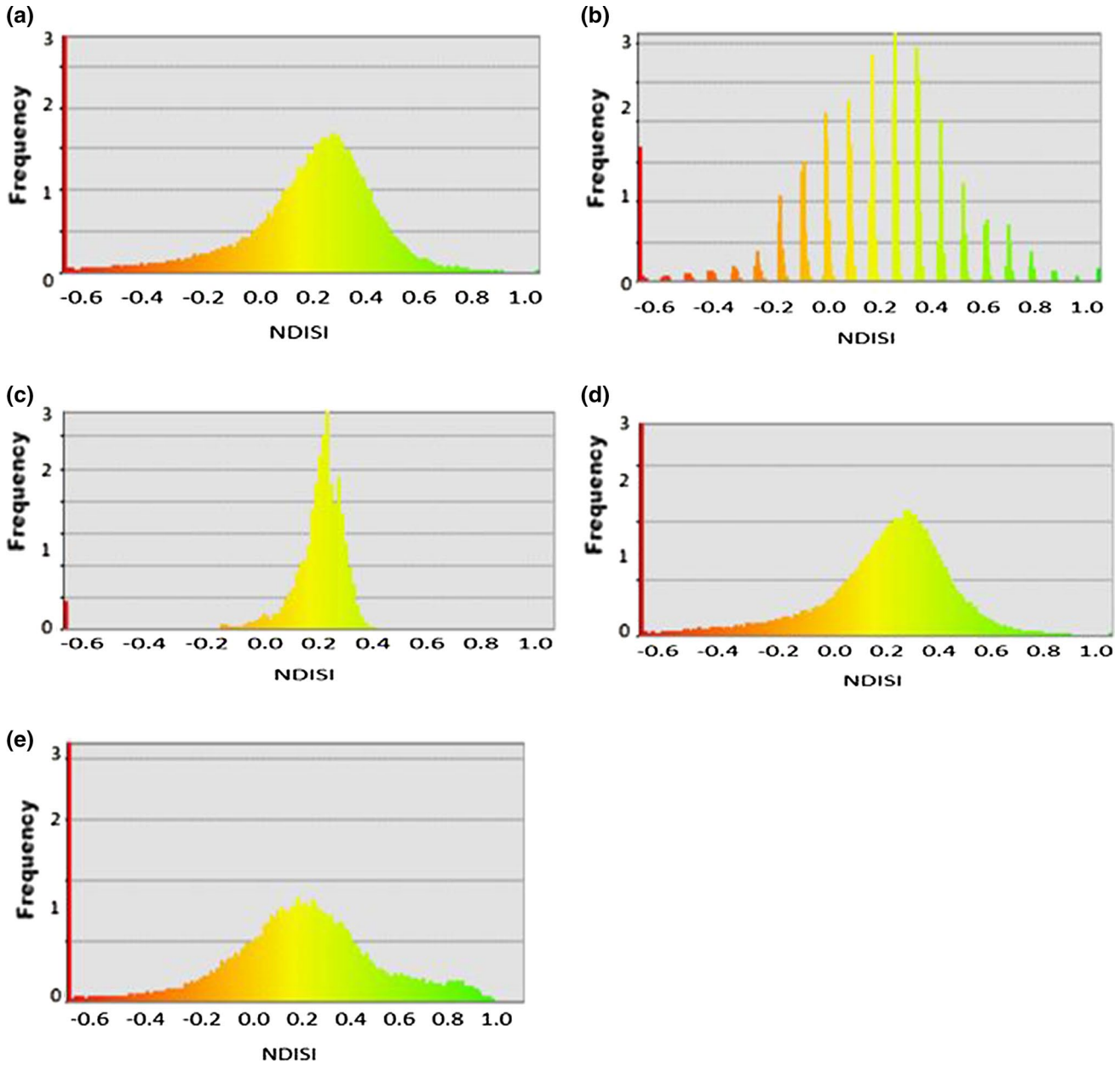

Fig. 8 Histograms of NDISI for different years **a** 1984, **b** 1994, **c** 2004, **d** 2014 and **e** 2019

of NDISI, which revealed that the area has an abundance of vegetation in that year. It was noted that different choices can be made for the visible band for the evaluation of NDISI, and therefore, other indices, such as GEMI, have been evaluated for comparison in this study to detect the degree to which the area has deteriorated over the time.

In order to further investigate the ability to distinguish between impervious surfaces and non-impervious surfaces, index values were determined for five land-use/land-cover dynamics, and a strong difference in quality between NDISI and land feature dynamics can be found (Fig. 2). Of note is that NDISI values are approximately equal to or less than zero for most vegetation and other land-cover pixels, whereas impervious surfaces have positive and high NDISI values. It is, therefore, observed that these histograms have a narrow range, indicating a high level of distinguishability between impervious surfaces and other land features. Although most of the histograms are separable, there are still small overlaps in the results for NDISI. A major difference between the analyses is NDISI's broader index value ranges of vegetation and bare soil (Figs. 7, 8), which shows a distinction between impervious and non-impervious surfaces.

This observation is supported by visual comparisons of the results of the indices for the study area which was chosen

to validate the dynamics of land-use/land-cover categories (Figs. 2, 7) and their patterns. Several non-impervious surface patches of NDISI results were found which were characterised by a green tone, while impervious covers were represented by yellow and red tones. The spatial trends of impervious and non-impervious surfaces in the study area could be attributed to the degradation patterns or extent during the selected years as indicated from studies conducted by Beck et al. (2016) and Xin et al. (2020). Various patterns observed in the studied period also connote that the land-use/land-cover dynamics or the degraded areas vary with years. For instance, the year 1984 has a less or moderate impervious surface, while 1994, 2004, 2014 and 2019 have high NDISI values in most parts of the study area. This shows the variability or spatial patterns of land features and their associated level of land degradation in the mining area. Although impervious surfaces may affect water quality, environmental health and ecosystem services (Beck et al. 2016; Xin et al. 2020), its spatial coverage and suitability to monitor degradation patterns may not be able to ascertain the actual impacts of mining activities on the environment and its related systems. Findings obtained from this study need to be complemented with physical measurement on the ground to be able to quantify and identify the type and extent of the impact. The outcome of this study provides a cost-effective tool for evaluating land use/land cover and change in mining areas that can drive policy interventions for remediation in affected areas.

Conclusion

Mining process is one of the human activities that can change the entire landscapes, accompanied by a variety of implications. This study presents the current trend of landscape dynamics in Welkom between 1984 and 2019 using Landsat images. The result from the study shows the recent changes and how it evolved over the years where tailings dam and built-up, effluent and water bodies increased in some of the years. More importantly, the area experienced increased vegetation from 342.5 to 371.1 km^2 during the period of study, which connotes that some parts of the study area were revegetated during those years. The status of the vegetation health in the area through the use of some vegetation indices such as Normalised Difference Moisture Index (NDMI), Normalised Difference Impervious Surface Index (NDISI) and Global Environmental Monitoring Index (GEMI) was established. These indices also revealed the spatial–temporal patterns of different land-use/land-cover dynamics. For instance, the area with low or negative values in GEMI and NDISI connotes low vegetation or degraded zone, while the areas with − 1 or zero values of NDMI reveal less vegetated zones or areas that are prone to environmental injustices due to mining operations and other human activities.

Consequently, continuous monitoring of the transformation of the different land-use/land-cover classes is important for implementing environmental management programmes that will advance sustainability in mining. The findings will also help in taking proactive measures in appraising and enforcing mining and development laws to manage and limit the fast depletion of the natural land cover within the study area and other mining areas. The results can also be communicated to mining companies to inform them of the need to monitor their surrounding environment to determine the annual rates or changes in land cover due to their operations and propose ways to reclaim or rehabilitate lost vegetated and degraded areas. More so, since this study cannot be ascertained the extent of gold mining activities impact on the surrounding environments, to determine the management strategies for such impacts and changes, this study recommends on-site timely monitoring for an accurate impact identification.

Acknowledgement The authors are grateful to the Faculty of Natural and Agricultural Sciences Central Research Funding, University of the Free State South Africa (Grant Number: UFSCRF201901) and USGS for providing satellite data for the analysis.

Data availability statement Satellite data used in this study were obtained from the database of the United States Geological Survey (https://earthexplorer.usgs.gov/).

Compliance with ethical standards

Conflict of interest Authors declare that there is no conflict of interest.

References

Adefisan EA, Bayo AS, Ropo OI (2015) Application of geo-spatial technology in identifying areas vulnerable to flooding in Ibadan metropolis. J Environ Earth Sci 5(14):153–166

Bebbington A, Hinojosa L, Bebbington DH, Burneo ML, Warnaars X (2008) Contention and ambiguity: mining and the possibilities of development. Dev Change 39(6):887–914

Beck SM, McHale MR, Hess GR (2016) Beyond impervious: urban land-cover pattern variation and implications for watershed management. Environ Manag 58(1):15–30

Bolton DK, Friedl MA (2013) Forecasting crop yield using remotely sensed vegetation indices and crop phenology metrics. Agric For Meteorol 173:74–84

Bonham-Carter GF (1994) Geographical information systems for geoscientists: modeling with GIS. Computer methods in the geosciences, vol 13. Elsevier, Amsterdam

Brabyn L, Zawar-Reza P, Stichbury G, Cary C, Storey B, Laughlin DC, Katurji M (2014) Accuracy assessment of land surface temperature retrievals from Landsat 7 ETM+ in the Dry Valleys of Antarctica using iButton temperature loggers and weather station data. Environ Monit Assess 186(4):2619–2628

Busayo ET, Kalumba AM, Orimoloye IR (2019) Spatial planning and climate change adaptation assessment: perspectives from Mdantsane Township dwellers in South Africa. Habitat Int 90:101978

Chen K, Blong R, Jacobson C (2003) Towards an integrated approach to natural hazards risk assessment using GIS: with reference to bushfires. Environ Manag 31(4):0546–0560

Chen Y, Huang C, Ticehurst C, Merrin L, Thew P (2013) An evaluation of MODIS daily and 8-day composite products for floodplain and wetland inundation mapping. Wetlands 33(5):823–835

Du J, Kimball JS, Jones LA (2015) Passive microwave remote sensing of soil moisture based on dynamic vegetation scattering properties for AMSR-E. IEEE Trans Geosci Remote Sens 54(1):597–608

Glantz MH (2019) Desertification: environmental degradation in and around arid lands. CRC Press, Boca Raton

Granell C, Díaz L, Gould M (2010) Service-oriented applications for environmental models: reusable geospatial services. Environ Model Softw 25(2):182–198

Gumma MK, Mohanty S, Nelson A, Arnel R, Mohammed IA, Das SR (2015) Remote sensing based change analysis of rice environments in Odisha, India. J Environ Manag 148:31–41

Hardisky MA, Klemas V, Smart M (1983) The influence of soil salinity, growth form, and leaf moisture on the spectral radiance of *Spartina alterniflora*. Photogramm Eng Remote Sens 49:77–83

Haryani NS, Prasasti I, Fitriana HL, Priyatna M, Khomarudin MR (2018) Detecting the area damage due to coal mining activities using landsat multitemporal (Case Study: Kutai Kartanegara, East Kalimantan). Int J Remote Sens Earth Sci 14(2):151–158

Heggelund G, Andresen S, Ying S (2005) Performance of the global environmental facility (GEF) in China: achievements and challenges as seen by the Chinese. Int Environ Agreem Politics Law Econ 5(3):323–348

Hou XY, Liu SL, Cheng FY, Zhang YQ, Dong SK, Su XK, Liu GH (2019) Vegetation community composition along disturbance gradients of four typical open-pit mines in Yunnan Province of southwest China. Land Degrad Dev 30(4):437–447

Howell DC (2002) Statistical methods for psychology. Wiley, New York

Karan SK, Samadder SR, Maiti SK (2016) Assessment of the capability of remote sensing and GIS techniques for monitoring reclamation success in coal mine degraded lands. J Environ Manag 182:272–283

Li J, Song C, Cao L, Zhu F, Meng X, Wu J (2011) Impacts of landscape structure on surface urban heat islands: a case study of Shanghai, China. Remote Sens Environ 115(12):3249–3263

Li LC, Deng L, Cao Y, Xiao WJ, Chen CY, Li HZ (2012) Vegetation dynamic monitoring in mining area based on NDVI serial images and dimidiate pixel model. J Central South Univ For Technol 32(6):18–23

Li S, Di X, Wu D, Zhang J (2013) Effects of sewage sludge and nitrogen fertilizer on herbage growth and soil fertility improvement in restoration of the abandoned opencast mining areas in Shanxi, China. Environ Earth Sci 70(7):3323–3333

Li Y, Jia Z, Sun Q, Zhan J, Yang Y, Wang D (2016) Ecological restoration alters microbial communities in mine tailings profiles. Sci Rep 6:25193

Liu C, Shao Z, Chen M, Luo H (2013) MNDISI: a multi-source composition index for impervious surface area estimation at the individual city scale. Remote Sens Lett 4(8):803–812

Liu Y, Wang Y, Peng J, Du Y, Liu X, Li S, Zhang D (2015) Correlations between urbanization and vegetation degradation across the world's metropolises using DMSP/OLS nighttime light data. Remote Sens 7(2):2067–2088

Maya M, Musekiwa C, Mthembi P, Crowley M (2015) Remote sensing and geochemistry techniques for the assessment of coal mining pollution, Emalahleni (Witbank), Mpumalanga. S Afr J Geomat 4(2):174–188

Mensah E, Wapaburda S, Hammond F (2017) A hybrid image classification approach to monitoring LULC changes in the mining District of Prestea-Huni Valley, Ghana. J Environ Earth Sci 7(3):1–10

Mudd GM (2010) Global trends and environmental issues in nickel mining: sulfides versus laterites. Ore Geol Rev 38(1–2):9–26

Mutukwa SBV, Ololade OO, Sokolic F (2019) Characterisation of invasive plant proliferation within remnant riparian green corridors in Lusaka District of Zambia using Sentinel-2 imagery. Remote Sens Appl Soc Environ 15:100245

Ololade O, Annegarn HJ, Limpitlaw D, Kneen MA (2008) Land-use mapping and change detection in the rustenburg mining region using landsat images. In: Proceedings of the IEEE international geoscience and remote sensing symposium IGARSS 08, 6-11 July 2008, Boston, MA. IV, pp 818–821

Orimoloye IR, Ololade OO (2020a) Potential implications of gold-mining activities on some environmental components: a global assessment (1990 to 2018). J King Saud University-Sci 32(4):2432–2438

Orimoloye IR, Ololade OO (2020b) Global trends assessment of environmental health degradation studies from 1990 to 2018. In: Environment, development and sustainability: a multidisciplinary approach to the theory and practice of sustainable development. Springer, pp 1–14

Orimoloye IR, Mazinyo SP, Nel W, Kalumba AM (2018) Spatiotemporal monitoring of land surface temperature and estimated radiation using remote sensing: human health implications for East London, South Africa. Environ Earth Sci 77(3):77

Perumal K, Bhaskaran R (2010) Supervised classification performance of multispectral images. arXiv preprint arXiv:1002.4046

Pinty B, Verstraete MM (1992) GEMI: a non-linear index to monitor global vegetation from satellites. Vegetatio 101(1):15–20

Porwal A, Carranza EJM (2015) Introduction to the special issue: GIS-based mineral potential modelling and geological data analyses for mineral exploration. Ore Geol Rev 71:477–483

Sebego RJ, Atlhopheng JR, Chanda R, Mulale K, Mphinyane W (2019) Land use intensification and implications on land degradation in the Boteti area: Botswana. Afr Geograph Rev 38(1):32–47

Sheoran V, Sheoran AS, Poonia P (2010) Soil reclamation of abandoned mine land by revegetation: a review. Int J Soil Sediment Water 3(2):13

Werner TT, Bebbington A, Gregory G (2019) Assessing impacts of mining: Recent contributions from GIS and remote sensing. Extr Ind Soc 6(3):993–1012

Willie YA, Pillay R, Zhou L, Orimoloye IR (2019) Monitoring spatial pattern of land surface thermal characteristics and urban growth: a case study of King Williams using remote sensing and GIS. Earth Sci Inf 12:1–18

Winde F, Hoffmann E, Espina C, Schüz J (2019) Mapping and modelling human exposure to uraniferous mine waste using a GIS-supported virtual geographic environment. J Geochem Explor 204:167–180

Xie L, Li G, Xiao M, Peng L (2016) Novel classification method for remote sensing images based on information entropy discretization algorithm and vector space model. Comput Geosci 89:252–259

Xie H, He Y, Xie X (2017) Exploring the factors influencing ecological land change for China's Beijing–Tianjin–Hebei Region using big data. J Clean Prod 142:677–687

Xin HANG, Yachun LI, Xiaochun LUO, Min XU, Xiuzhen HAN (2020) Assessing ecological quality of Nanjing during its urbanization process by using satellite, meteorological, and socioeconomic data. J Meteorol Res 34(2):1–14

Zarin D, Alavalapati JR, Schmink M, Putz FE (eds) (2004) Working forests in the neotropics: Conservation through sustainable management?. Columbia University Press, New York

Zhang J, Rao Y, Geng Y, Fu M, Prishchepov AV (2017) A novel understanding of land-use characteristics caused by mining activities: a case study of Wu'an, China. Ecol Eng 99:54–69